Article

JOURNAL OF REINFORCED PLASTICS & COMPOSITES

Journal of Reinforced Plastics and Composites
30(4) 325–335

DOI: 10.1177/0731684410396599
jrp.sagepub.com

SAGE

Effect of the polymer–filler interaction on the thermo-mechanical response of polyurethane–clay nanocomposites from blocked prepolymer

Andrea Dorigato, Alessandro Pegoretti and Amabile Penati

Abstract

Thin transparent films of polyurethane–clay nanocomposites were prepared by dispersing different amounts of commercial organo-modified clay in a mixture of cycloaliphatic amines used as chain extender of a blocking prepolymer, in order to investigate the role of the filler content on the thermo-mechanical behavior of the resulting composites. X-ray diffraction measurements evidenced the formation of an intercalated structure, regardless to the clay loading. Furthermore, the optical clarity of the samples was not substantially compromised by the nanofiller addition even at elevated clay amounts. Interestingly, the relatively strong polymer–filler interaction led to a substantial reduction of the matrix crosslinking degree for high clay loadings. Consequently, the relative thermal lifetime was positively affected by the presence of clay up to a filler content of 7 wt%, while uniaxial tensile tests under quasi-static and impact conditions evidenced an increase of the elastic modulus proportional to the clay concentration, without impairing the original tensile properties at break.

Keywords

polyurethane, clay, nanocomposites, mechanical properties, thermal properties

Introduction

Polymer–clay nanocomposites represent one of the most promising classes of materials of the last decades. Starting from the PA6/clay nanocomposite patented by Toyota for automotive applications,[1–4] many efforts have been made to develop nanocomposite systems, utilizing different polymeric matrices and various kinds of nanofillers.[5–11]

Polyurethanes (PUs) present a unique combination of high performances and relatively simple production process. Because of the great variety of chemical reagents available for their synthesis (macrodiols, diisocyanates, chain extenders, and crosslinkers), PUs are probably the most versatile class of polymer.[12] Chattopadhyay and Raju[13] recently reviewed the history and the modern trends in the preparation of high performance polyurethanes. One of the most interesting industrial application of PUs is represented by the production of organic coatings having aesthetic appearance and corrosion protection to be applied on metallic substrates.

In the last few years, many efforts have been made for the improvement of the thermo-mechanical properties of elastomeric polyurethanes by the introduction of small amounts of inorganic nanostructured materials.[14–57] Among nanofiller that could be added to polymeric matrices, organo-modified clays were most frequently utilized because of their relatively low cost and high effectiveness. Montmorillonites are sodic

Department of Materials Engineering and Industrial Technologies, University of Trento, Italy.

Corresponding author:
Andrea Dorigato, Department of Materials Engineering and Industrial Technologies, University of Trento, via Mesiano 77, 38123, Trento, Italy
Email: andrea.dorigato@ing.unitn.it

aluminum hydrosilicates characterized by a lamellar crystalline structure, in which every layer (1 nm thick and 100–200 nm wide) is constituted by alumina octahedra interposed between two silica tetrahedra. The lamellae are weakly bonded together through van der Waals forces. The sodium montmorillonite presents negatively charged layers, because of the presence of some Al/Mg and Si/Al substitutions, and positively charged interlayer domains, for the presence of sodium ions. Organophilic montmorillonites, to be used in combination with hydrophobic polymers (such as PE or PP), can be prepared through the substitution of Na^+ ions with cations of quaternary ammonium salts.

In 1998 Wang and Pinnavaia[58] presented the first study on PU/clay nanocomposites, in which a fully exfoliated material, maintaining a good optical transparency and improving the tensile properties of the pristine matrix, was obtained. From that moment many efforts were made to synthesize novel PU/clay nanocomposite systems. Considering literature references, the improvements due to nanoclay introduction in polymers are generally related to an enhancement of their elastic modulus,[15,17,19,21,22,24,28,36,37,45,58] of their tensile strength,[17,24,28,34–36,54,56,58] of their tensile strain at break,[17,24,28,34–36,54,56,58] of their storage modulus,[21,28,41,44,46,56] of their Shore hardness,[28] and tear strength.[24] In some cases, nanofiller agglomeration led to a significant reduction of the material toughness, with a strong reduction of tensile stress at break[21,22,34,45] and strain at break.[15,21,22,28,45] In some papers, a non-monotonic trend of the mechanical properties as function of the clay type[14] and content[22,30,33,49,52] has been reported. Furthermore, it can be frequently found that also the thermal degradation resistance[16–19,30,35,42,44,59] and the barrier properties[19,23,45] can be improved by the clay addition. If the clay dispersion in the PU matrix is obtained at an optimal level, the optical clarity of the PU coating[15,35] can be maintained and the corrosion protection of the substrates[17,18] can be in some cases improved.

Many efforts were also devoted to the synthesis of novel PU/clay nanocomposites by using different preparation routes. In most cases, organoclays have been dispersed into the polyol and the mixture was then crosslinked by using a diisocyanate and a chain extender[28,29,31,40,43,45,49,50,52,54,56] or a prepolymer.[42] Alternatively, the organoclays have been dispersed in the prepolymer,[17,33–35,44] or directly in the PU matrix by solvent[14,16,18,19,21,22,24] or melt [15,22,35,36] procedures. A latex compounding route to add a sodium hectorite to polyurethane rubber was also reported by Varghese et al.[46]

It was recently demonstrated that blocked polyisocyanates could be quite effective for the production of PU coatings in which stable formulations at room temperature are required. In these conditions the curing reactions could be conducted after the application of the coatings on metallic substrates by fast thermal treatments.[12] The reactivity of these oligomers, also called end-capped or masked polyisocyanates, is related to the ability of the urethane group to be thermally decomposed. The most frequently utilized isocyanate masking agents are phenol, caprolactam, malonate, methyl-ethyl ketoxime, isophenol, and many others. Quite surprisingly, only little attention has been devoted to the synthesis of PU-based nanocomposites from blocked polyisocyanates.[49,60]

The suitability of PU coatings obtained from prepolymers blocked with MEKO (methyl-ethyl-ketoxime) and the possibility to utilize this matrix in the preparation of PU–clay nanocomposites was recently investigated by our research group.[61] In particular, the efficacy of the vibration induced equilibrium contact angle (VIECA) technique to assess a quantitative estimation of the clay hydrofobicity[62] was evaluated. The intercalation degree of the clays dispersed in PU matrix obtained from a blocked prepolymer resulted to be strongly related to the water–clay equilibrium contact angle of the selected organoclays. The PU crosslinking degree decreased as the clay–filler interaction improved. Moreover, thermo-mechanical properties showed a non-monotonic trend as a function of the intercalation degree, showing a maximum. This behavior was explained considering that two concomitant and contrasting effects develop as the polymer–clay intercalation degree increases: a positive improvement of the filler matrix interactions, and a negative reduction of the matrix crosslinking degree. Consequently, an optimum balance between the above reported contrasting effects was reached by using a middle hydrophobicity (Cloisite® 25 A) clay.

Starting from these considerations, in this work we prepared PU–clay nanocomposites by using different amounts of Cloisite® 25 A clay, in order to assess the effect of the clay loading and of the polymer–filler interaction on the microstructural and thermo-mechanical properties of the resulting composites, with particular attention to their thermal degradation resistance and to their tensile mechanical response under quasi-static and impact conditions.

Experimental

Materials

The polyurethane matrix utilized in this article was a commercial partly cross-linked polyurethane, supplied by API – Applicazioni Plastiche Industriali SpA (Vicenza – Italy), based on a blocked polyurethane

prepolymer, obtained by MDI (2,4′ diphenylmethane-diisocyanate) and a trifunctional polyether polyol (average molar mass = 4700 g·mol^{-1}, OH content = 34–38 mgKOH·g^{-1}). The prepolymer had an ambient temperature viscosity of 110 Pa·s and was end-capped by a methyl-ethyl-ketoxime (MEKO). The chain extender-crosslinker was a mixture of cycloaliphatic amines (density = 0.945 g·cm^{-3}, weight average molar mass = 230–250 g·mol^{-1}, viscosity at 20°C = 170 mPa·s). As explained in the introduction, an organo-modified (Cloisite® 25 A) clay, provided by Southern Clay Products, Inc. (Gonzales, Texas), was chosen for the preparation of the composites. Some physical and chemical properties of this organoclay are reported in Table 1.

Composites manufacturing

The selected clay was mechanically dispersed in the chain extender at room temperature by using a Dispermat F1 mixer rotating at 2000 rpm for 5 min. The choice of dispersing the clays in the chain extender was related to its lower viscosity and to a higher polarity with respect to the prepolymer. The mixture was then ultrasonicated at room temperature in a Transsonic 460/H device at 35 kHz for 5 min. The prepolymer was added to the chain extender-clay mixture at room temperature through mechanical dispersion for 5 min at 2000 rpm. According to the producers' indications, a prepolymer/chain extender ratio equal to 88/12 was adopted. The mixture was then poured on a non-stick silicon paper and filmed trough a semi-automatic doctor blade device. Prepolymer unblocking and reaction with the chain-extender/crosslinking agent was finally promoted by a thermal treatment at 160°C for 2 min, in order to obtain uniform films with a mean thickness of 0.5 mm. In this way PU–clay nanocomposites at different filler loadings (1, 3, 5, 7, 10 wt%) were prepared. The pure matrix was denoted as PU, while the nanocomposites were designated with the name of the matrix (PU), followed by the type of clay (25 A) and by the filler concentration. For example, PU-25 A-5 indicated the nanocomposite sample filled with 5 wt% of Cloisite® 25 A clay.

Testing procedures

X-ray diffraction analyses were performed through a HRD 3000 high resolution diffractometer (Ital Structures, Italy) with a radiation wavelength of 0.15406 nm, an initial 2θ angle of 1°, and a 2θ increment of 0.05°. Utilizing the Bragg's law, it was possible to evaluate the interlamellar spacing values of the original clay (d_0) and of the clay in the composites (d). The intercalation degree (ID) could be therefore defined as follows:[63]

$$ID = \frac{d - d_0}{d_0} \quad (1)$$

Digital pictures for the evaluation of the optical transparency of the specimens were collected by a Nikon Coolpix 4500 digital camera at a distance of 30 cm from the specimen. ESEM images of the cryo-fractured surfaces of the nanocomposites were collected by using a Philips XL30 (Hillsboro, Oregon, USA) environmental scanning electronic microscope (ESEM), at an acceleration voltage of 10 kV and a magnification of 500×.

The estimation of the crosslinking degree was performed by measuring the amount of polymer matrix that could be extracted by immersion in N,N-dimethyl-formamide (DMF). Specimens were immersed in DMF for 24 h, and a thermal treatment under vacuum at 50°C for 8 h was then carried on, in order to remove the solvent. Considering the mass of the specimens before (m_b) and after (m_a) the solvent extraction procedure, a crosslinking degree (CD) was estimated as follows:

$$CD = \frac{m_a}{m_b} \quad (2)$$

Table 1. Organoclays utilized in this study. Information taken from the producer data sheets

Trade name	Organic modifier	Modifier concentration (meq·(100 g)$^{-1}$)	Density (g·cm^{-3})	d_{001} spacing (nm)
Cloisite® 25A	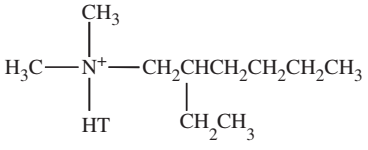	95	1.87	1.86

T = Tallow (~65% C18; ~30% C16; ~5% C14) and HT is Hydrogenated Tallow.
Anion: chloride.

Thermogravimetric analyses (TGA) were performed by a Mettler TG50 furnace (Schwerzenbach, Switzerland), connected to a Mettler MT5 balance and a Mettler TC 10 A unit control. The measurements were conducted in isothermal mode, at a constant temperature of 250°C under a nitrogen flow of 100 mL·min^{-1}. A lifetime was estimated in correspondence of a 3 wt% mass loss (called $t_{0.03}$).

Both quasi-static and impact tensile mechanical properties were measured on ISO 527 type 1BA dumbbell specimens punch cut from the polyurethane films. Specimens had a width of 5 mm and a gage length of 30 mm. Quasi-static tensile tests were performed by an Instron model 4502 testing machine (Norwood, MA, USA) equipped with a load cell of 100 N at a crosshead speed of 50 mm·min^{-1}. Axial strain was evaluated by an Instron model 2603-080 long travel elastomeric extensometer with a gage length of 25 mm. At least five specimens were tested for each sample. Tensile impact tests were conducted by a CEAST model 6549 instrumented pendulum (Turin, Italy) in tensile configuration, connected to a Ceast DAS-4000 data acquisition unit. All the tests were performed at a striking speed of 1 m·s^{-1} and with at a impact energy of 1.08 J. At least five specimens were tested for each sample.

Results and discussion

Microstructure and morphology

X-ray diffraction patterns of pure Cloisite® 25 A clay and of the nanofilled samples are reported in Figure 1, while in Table 2 interlamellar distances of the clay powder (d_0) and of the clay in the composites (d), with the relative intercalation degree (ID) values, are summarized. From the diffractograms it is evident the presence of well defined diffraction peaks, whose intensity was proportional to the filler content. This means that the original crystalline order of the clay nanoplatelets was maintained also in the composites. Comparing the diffraction signal of the pure clay with that of the nanofilled samples, a shift of the characteristic peak toward lower angles could be detected. The interlamellar distance passed from 1.88 nm of the as-received clay to about 2.90 nm of the nanocomposites, with a relative ID of about 55%. Considering that the position of the diffraction signal was not influenced by the clay loading, it can be concluded that an intercalated structure has been obtained for all the composites, and that the intercalation degree was independent from the filler content. Even if in several papers on PU-based nanocomposites the complete exfoliation of the clay nanoplatelets has been reached,[64,65] also the simple intercalation of the lamellae was frequently reported in literature.[66–70]

Even if the complete disruption of the original crystalline order of the nanoclay was not reached, the transparency of the nanocomposites to visible light resulted satisfactory for coating applications, as documented in Figure 2. As commonly reported in literature references on polymer–clay nanocomposites,[71,72] the relative transparency of the nanocomposites slightly decreased with the clay content, but the optical clarity of the coat was not seriously compromised even at high filler loadings.

ESEM images of cryo-fractured surfaces of the pure PU and of the relative nanocomposites are reported in Figure 3. The surface of the unfilled matrix appeared flat and uniform, with the presence of some spherical holes with a mean size of 50 μm, probably due to the oxime evaporation during the chain extension process. The introduction of the clay modified the fracture profile, with an increase of the surface roughness with the clay concentration. It is generally believed that the surface roughening due to presence of the nanofillers could be responsible of an enhancement of the material

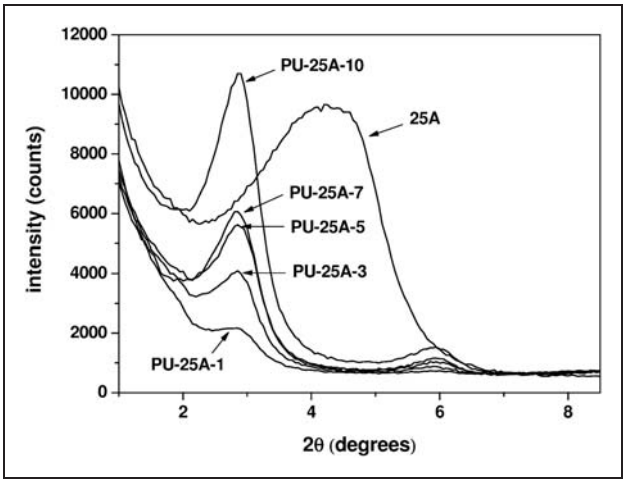

Figure 1. X-Ray diffractograms of pure Cloisite® 25 A clay and relative PU–clay nanocomposites.

Table 2. Interlamellar distances and intercalation degree of pure Cloisite® 25 A clay and relative PU-clay nanocomposites from X-ray diffraction measurements tests

Sample	d (nm)	d_0 (nm)	ID (%)
25 A	–	1.88 ± 0.02	–
PU-25 A-1	2.92 ± 0.03	–	55.1
PU-25A-3	2.94 ± 0.01	–	56.3
PU-25 A-5	2.90 ± 0.01	–	54.1
PU-25 A-7	2.92 ± 0.01	–	55.1
PU-25 A-10	2.92 ± 0.01	–	55.1

fracture toughness.[73–75] As will be discussed below, the introduction of clay in these systems led only to a slight improvement in their tensile properties at break.

Crosslinking degree values of pure PU matrix and of the relative nanocomposites, evaluated according to Equation (2), are summarized in Figure 4. While the unfilled sample showed a CD value of 92.6%, the introduction of the clay led to a decrease of the crosslinking degree of the material. Even if the CD drop was practically negligible up to a clay concentration of 7 wt%, a more significant decrease could be registered for PU-25 A-10 sample. Even if further investigations should be necessary to interpret this behavior, a tentative explanation could be provided. According to sample preparation technique, the nanofiller was preliminary dispersed in the chain extender-crosslinker, because of its lower viscosity. Therefore, as the clay amount increased, more and more chain extender-crosslinker was probably segregated between the interlamellar galleries of the clay, where it could be hardly reached by the more viscous prepolymer. The presence of unreacted prepolymer and chain extender-crosslinker could explain lower crosslinking degree values displayed by highly filled nanocomposites. A similar explanation was already proposed in our previous work on PU–clay nanocomposites.[62] In that case, the heavy reduction of the matrix crosslinking degree displayed by the composites filled by the most hydrophilic clays (Cloisite® 30B) was ascribed to the strong polymer–filler interfacial interaction that led to the absorption of high amounts of chain extender in the intragallery spaces, with detrimental effects on the crosslinking kinetics of the material. Also, Kim et al.[76] studying the effect of molecular weight on the adhesion properties of polyurethane/lamellar silicate nanocomposites, found that the crosslinking of the PU matrix was reduced by the presence of Cloisite® 30B clay. They hypothesized that the increased viscosity of the nanofilled systems might be a cause of this decreased crosslinking degree. The reduced NCO content of the PU prepolymer induced by the reaction between the isocyanate group and clay organomodifier was suggested as another possible cause. The negative influence of the nanofiller introduction on the crosslinking process can be also found in some papers on other thermosetting nanocomposite systems. Akbari and Bagheri,[73] investigating the deformation mechanism of epoxy–clay nanocomposite under compressive and flexural loadings, detected from DSC tests on nanofilled samples the presence of a glass transition temperature about 20°C lower than the main transition of the neat matrix. It was hypothesized that alkylammonium ions might react with to epoxy monomers prior to the curing agent addition. During the curing process it was therefore possible that the gelation time was rather short and the crosslinker molecules did not have enough time to diffuse into clay galleries. Therefore, the occurrence of the second transition was attributed to the presence of an epoxy matrix with a lower crosslinking density, induced by epoxy macromolecules entrapped between the silicate galleries.

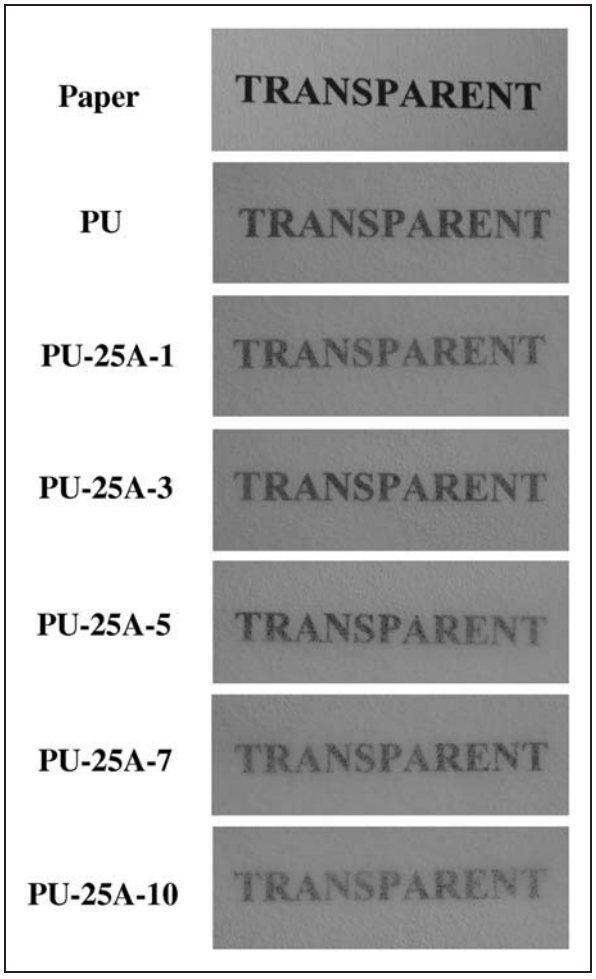

Figure 2. Optical transparency of neat polyurethane matrix and PU–clay nanocomposites.

Thermal stability

In Figure 5(a) isothermal thermogravimetric traces collected at 250°C for the unfilled matrix and for the relative nanocomposites are reported; while in Figure 5(b) thermal lifetime values associated to a mass loss of 3 wt% ($t_{0.03}$) are summarized. It could be inferred that the introduction of the clay had a positive effect on the thermal stability of the sample, with a general enhancement of $t_{0.03}$ values with respect to the unfilled matrix. As an example, for PU-25 A-7 sample an enhancement of the $t_{0.03}$ value of 57% was registered. As reported in literature references,[16,18,19,30,42] the

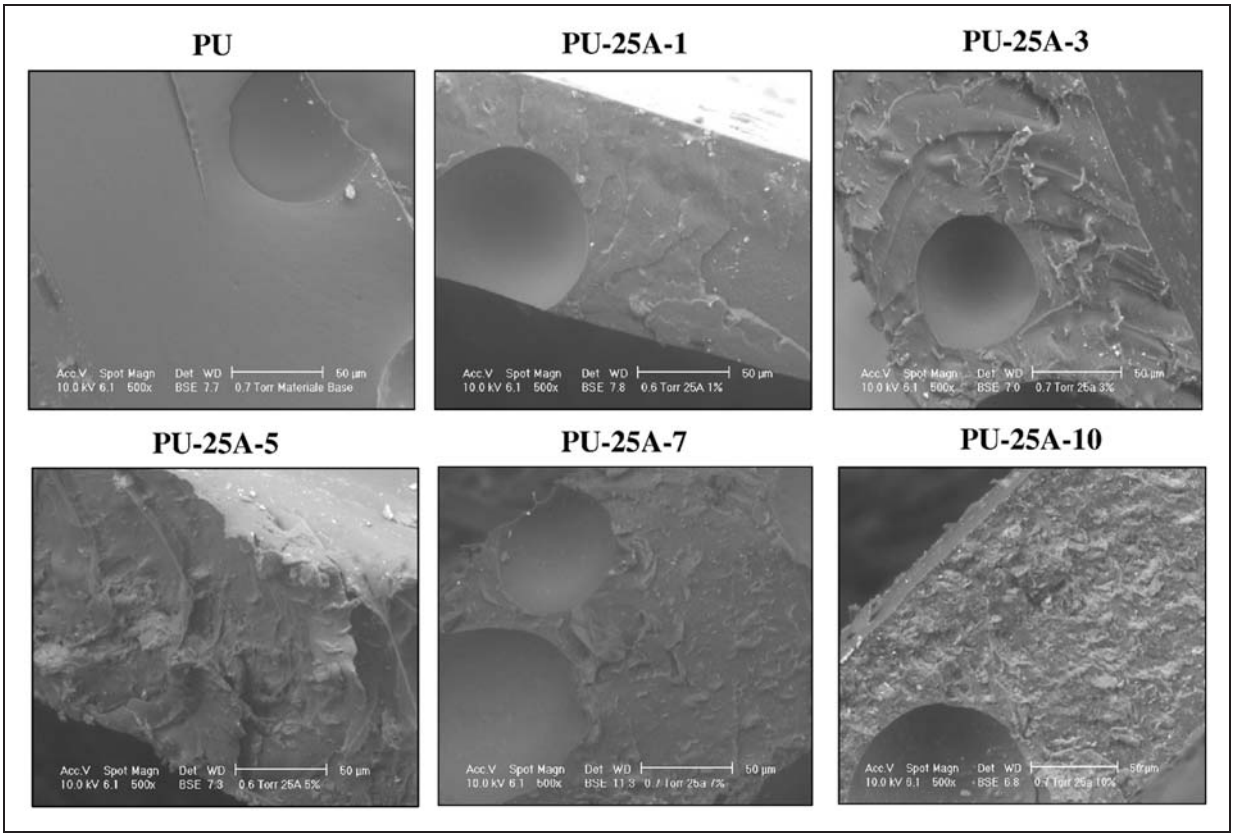

Figure 3. ESEM images of cryo-fractured surfaces of PU–clay nanocomposites.

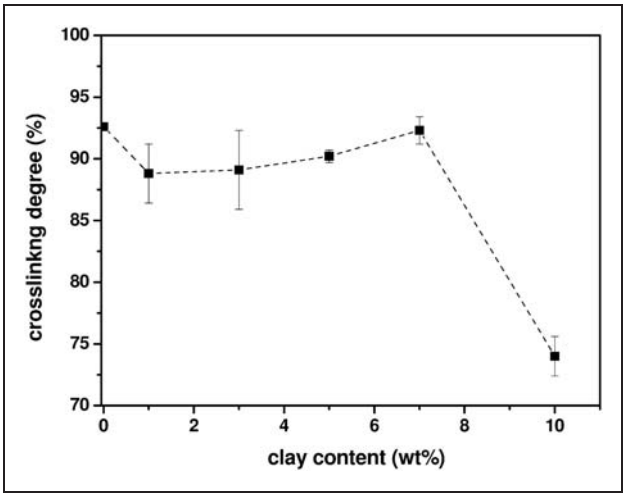

Figure 4. Relative crosslinking degrees of PU–clay nanocomposites from insoluble residue evaluation.

improvement of the degradation resistance could be probably related to the formation of a char layer in the material, limiting the diffusion of the oxygen through the sample and thus inhibiting the combustion process. It is also clear that the ability to form a protective shield against oxygen diffusion depends on the capability of clay tactoids to collapse on each other thus forming a continuous barrier. Increasing the filler amounts, it is likely that the mean distance between clay lamellae was considerably reduced, and the formation of a thicker and stronger shield was therefore favored. For high clay concentrations (10 wt%), the resistance to thermal degradation started to heavily decrease, probably because of the strong crosslinking degree drop detected at elevated filler amounts.

Mechanical behavior

In Figure 6, representative stress–strain curves of PU and of PU-25 A-7 nanocomposite under quasi-static and impact conditions are compared, while in Table 3 the most important quasi-static tensile properties are summarized. Regardless of the testing rate, the tensile behavior of the tested samples was typical of an elastomeric material in its rubbery state.[77] Unlike metals this stress-strain curve showed no (or considerably limited) linear portion. Therefore, it would have been not practical to calculate Young's modulus, intended as the slope of a straight line drawn tangent to the curve and passing through the origin. Instead, secant moduli, evaluated as the stress levels at selected elongations (50% and 100%), were reported.

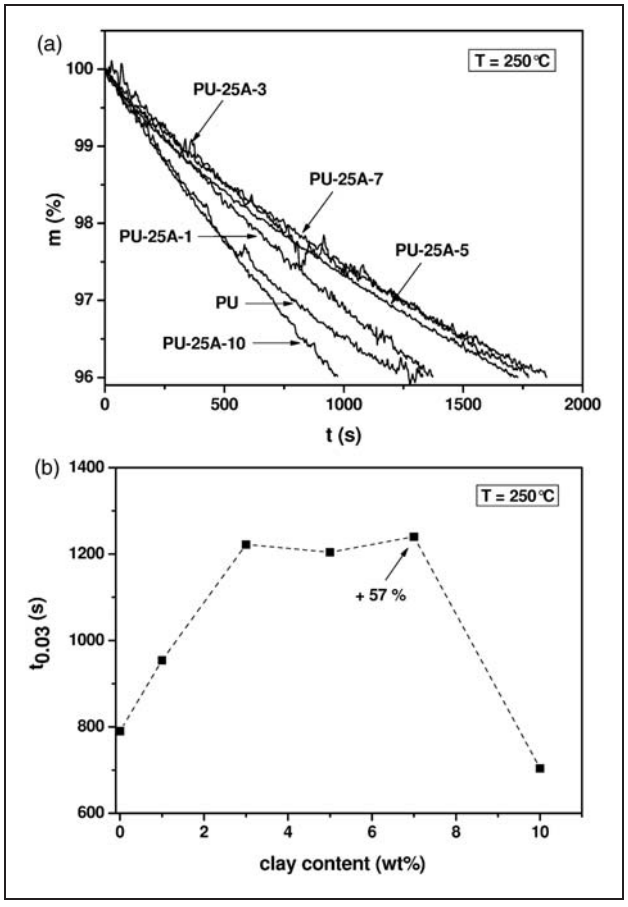

Figure 5. Thermogravimetrical analysis on PU and relative PU–clay nanocomposites: (a) isothermal thermogravimetric curves at 250°C, (b) lifetime for 3 wt% mass loss ($t_{0.03}$).

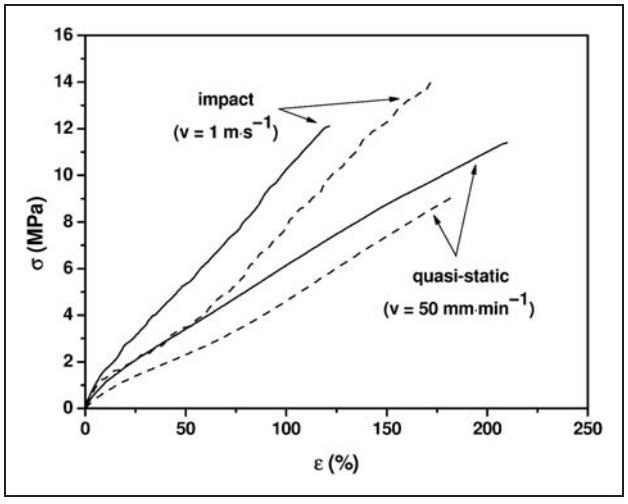

Figure 6. Representative stress–strain curves of PU samples (dashed line) and PU-25 A-7 nanocomposite (continuous line) in tensile mechanical tests under quasi-static and impact conditions.

Table 3. Quasi-static tensile properties of pure PU and relative PU-clay nanocomposites ($v = 50$ mm·min^{-1})

Sample	$E_{50\%}$ (MPa)	$E_{100\%}$ (MPa)	σ_b (MPa)	ε_b (%)
PU	4.6 ± 0.4	4.6 ± 0.5	9.7 ± 1.7	196 ± 37
PU-25 A-1	4.9 ± 0.7	4.9 ± 0.7	9.3 ± 1.9	180 ± 23
PU-25 A-3	5.2 ± 0.4	5.0 ± 0.3	8.8 ± 0.5	186 ± 18
PU-25 A-5	6.1 ± 0.3	5.9 ± 0.3	9.5 ± 1.6	170 ± 16
PU-25 A-7	6.7 ± 0.9	6.1 ± 0.7	10.1 ± 0.9	180 ± 17
PU-25 A-10	6.8 ± 0.4	5.6 ± 0.3	9.0 ± 0.8	205 ± 12

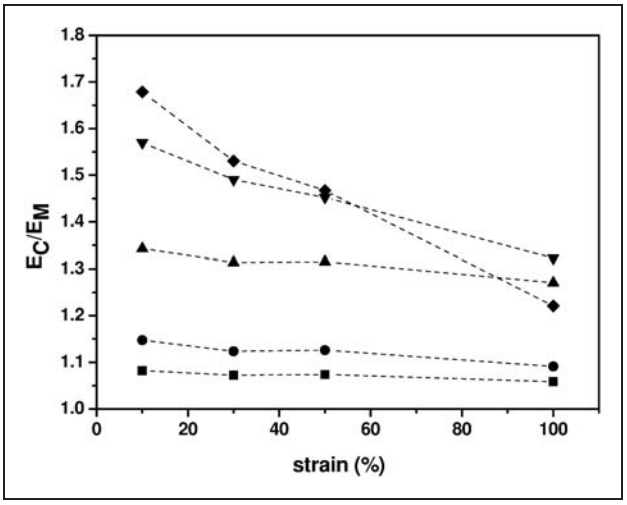

Figure 7. Secant elastic modulus increase vs. strain level of PU–clay nanocomposites from quasi-static tensile tests. PU-25 A-1 (■), PU-25 A-3 (●), PU-25 A-5 (▲), PU-25 A-7 (▼), PU-25A-10 (◆).

It is evident that the enhancement of the strain rate typical of the impact mechanical tests produced an embrittlement of the material, with an increase of the elastic modulus and of the stress at break, accompanied by a decrease of the strain at break. Quasi-static tensile properties at break (σ_b, ε_b) were substantially retained even at high filler contents, while the material stiffness increased with the clay concentration, probably because of the physical chain blocking mechanism provided by clay nanoplatelets. Even in this case the best mechanical performances were displayed by PU-25 A-7 composite, for which a $E_{50\%}$ enhancement of the 45% and a little increase of the stress at break were detected.

In Figure 7 relative elastic modulus values at different strain levels and for various filler loadings is reported. It is evident that the enhancement of elastic modulus with respect to the pure matrix was more evident at high clay concentrations and decreased with the deformation level. The best results were found for PU-25-10, for which an elastic modulus increase of 70% at a deformation level of 10% was registered.

Table 4. Tensile impact properties of pure PU and relative PU–clay nanocomposites ($v = 1\ m \cdot s^{-1}$)

Sample	$E_{50\%}$ (MPa)	$E_{100\%}$ (MPa)	σ_b (MPa)	ε_b (%)
PU	7.5 ± 0.7	7.6 ± 0.8	14.0 ± 1.3	170 ± 19
PU-25 A-1	7.3 ± 1.2	7.9 ± 1.2	10.9 ± 0.9	132 ± 18
PU-25 A-3	9.3 ± 1.5	9.4 ± 1.1	13.0 ± 1.9	141 ± 35
PU-25 A-5	10.6 ± 1.4	10.3 ± 0.9	14.5 ± 1.4	149 ± 16
PU-25 A-7	10.4 ± 0.5	9.8 ± 0.5	12.1 ± 1.2	126 ± 10
PU-25 A-10	13.2 ± 0.7	11.0 ± 0.8	12.4 ± 1.3	126 ± 17

The dependence of the viscoelastic properties of filled rubbers from the strain amplitude, often referred as the Payne effect,[78] has been extensively investigated in the last decades. The concept of filler networking yielded a good interpretation of the Payne effect for filled compounds.[79] According to this theory, the 3-D structure network constructed by filler aggregation might significantly alter the dynamic viscoelastic response of rubbers. The existence of this behavior in its physical meaning was correlated with the density and strength of a structure formed by the filler–filler interactions. Payne[80] hypothesized that the dependence of the moduli with strain was determined by the agglomeration and de-agglomeration of the filler network, that could be destroyed by the application of a strain of sufficient magnitude, leading to the loss of rigidity. At large deformation, the difference between unfilled and filled rubber was only determined by the contribution arising from the inclusion of rigid particles.[81] Recently, it was found that the modulus drop at high strain amplitude for rubber–clay nanocomposites could be also explained considering the breakdown of filler–rubber network constructed both by filler–filler interaction and by filler–rubber interaction.[82,83] Basing on experimental techniques at our disposal, it is difficult to assess if the stiffening effect provided by clay nanoplatelets at low strains was due to polymer–filler interaction rather than to filler networking. However, the presence of nanoclay greatly affected the elastic response of the prepared composites, and a strong dependence from the strain amplitude was detected.

The most important tensile impact properties of the pure PU matrix and of the relative nanocomposites are summarized in Table 4; while in Figure 8 the values of the specific energy adsorbed at different strain levels are collected. According to quasi-static tensile tests, impact elastic modulus increased with the clay content. As an example, an $E_{50\%}$ enhancement of the 77% with respect to the pure matrix could be detected for PU-25 A-10 composite. The increase of the elastic modulus at deformation of 50% and 100% was responsible of an enhancement of the specific energy values adsorbed at these strain levels. For instance, specific tensile energy

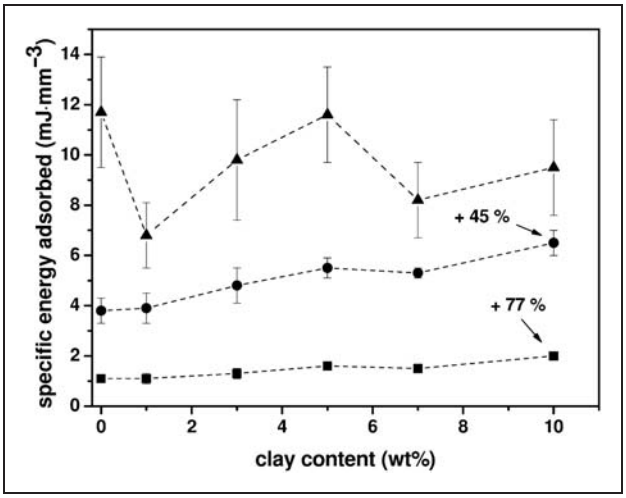

Figure 8. Specific energy adsorbed by pure PU and relative PU–clay nanocomposites in tensile impact tests at different strain levels. Strain = 50% (■), Strain = 100% (●), At break (▲).

adsorbed at 50% and of 100% strain from PU-25-10 composite were respectively 82% and 71% higher than that of the neat matrix. Moreover, from Table 4 it is also evident that the tensile properties at break were only marginally reduced with the nanofiller addition, with no clear dependence from the clay content. It can be therefore concluded that the original tensile energy adsorbed at break under impact conditions was practically unaffected by nanoclay introduction.

Conclusions

Different concentrations of organo-modified clay were dispersed in an amine chain extender of a blocked prepolymer, in order to prepare transparent elastomeric films of PU–clay nanocomposites, to be thermomechanically characterized.

Regardless to the filler content, X-ray diffraction analyses evidenced the formation on an intercalated structure, with an increase of the interlamellar spacing of the 55%. The good dispersion of the clay nanoplatelets allowed the nanocomposites to maintain the original optical clarity of the matrix at an acceptable level even at elevated filler concentrations. The crosslinking degree was considerably reduced at elevated clay concentrations, probably because the strong polymer–filler interaction negatively affected the cure kinetics of the resin. Consequently, the relative thermal lifetime of the nanofilled samples increased up to a clay content of 7 wt%, and then decreased

Elastic modulus was enhanced proportionally to the nanoclay content both under quasi-static and impact conditions, while the increase of the surface roughness with the clay content observed in ESEM images could explain the slight improvement of the tensile properties

at break detected for nanofilled samples in quasi-static tests.

Acknowledgment

The authors are grateful to Dr Antonio Petrone of API Spa for the provision of PU components.

Funding

This research received no specific grant from any funding agency in the public, commercial, or not-for-profit sectors.

References

1. Kawasumi M, Kohzaki M and Kojima Y. US Patent No. 4,810,7341989.
2. Kojima Y, Usuki A, Kawasumi M, Fukushima Y, Okada A and Kurauchi T. Mechanical properties of nylon 6-clay hybrid. *J Mater Res* 1993; 8(5): 1185–1189.
3. Okada A, Fukushima Y and Kawasumi M. US Patent No. 4,739,0071988.
4. Usuki A, Kawasumi M, Kojima Y, Fukushima Y, Okada A and Kurauchi T. Synthesis of nylon 6-clay hybrid. *J Mater Res* 1993; 8(5): 1179–1184.
5. Bondioli F, Dorigato A, Fabbri P, Messori M and Pegoretti A. High-density polyethylene reinforced with submicron titania particles. *Polym Eng Sci* 2008; 48: 448–457.
6. Bondioli F, Dorigato A, Fabbri P, Messori M and Pegoretti A. Improving the creep stability of high-density polyethylene with acicular titania nanoparticles. *J Appl Polym Sci* 2009; 112: 1045–1055.
7. Dorigato A and Pegoretti A. Tensile creep behaviour of poly(methylpentene)-silica nanocomposites. *Polym Int* 2010; 59: 719–724.
8. Dorigato A, Pegoretti A, Bondioli F and Messori M. Improving epoxy adhesives with zirconia nanoparticles. *Compos Interfaces* 2010; 17: 873–892.
9. Starkova O, Yang JL and Zhang Z. Application of time-stress superposition to nonlinear creep of polyamide 66 filled with nanoparticles of various sizes. *Compos Sci Technol* 2007; 67: 2691–2698.
10. Su S, Jiang DD and Wilkie CA. Poly(methyl methacrylate), polypropylene and polyethylene nanocomposite formation by melt blending using novel polymerically modified clay. *Polym Degrad Stab* 2004; 83: 321–331.
11. Zhao C, Qin H, Gong F, Feng M, Zhang S and Yang M. Mechanical, thermal and flammability properties of polyethylen/clay nanocomposites. *Polym Degrad Stab* 2005; 87: 183–189.
12. Schauerte K, Dahm M, Diller W and Uhlig K. Raw materials. In: Oertel G (ed.) *Polyurethane handbook*. Munich: Hanser Publishers, 1985, pp.42–116.
13. Chattopadhyay DK and Raju K. Structural engineering of polyurethane coatings for high performance applications. *Prog Polym Sci* 2007; 32(3): 352–418.
14. Chang JH and An YU. Nanocomposites of polyurethane with various organoclays: Thermomechanical properties, morphology, and gas permeability. *J Polym Sci Part B: Polym Phys* 2002; 40(7): 670–677.
15. Chavarria F and Paul DR. Morphology and properties of thermoplastic polyurethane nanocomposites: Effect of organoclay structure. *Polymer* 2006; 47(22): 7760–7773.
16. Chen TK, Tien YI and Wei KH. Synthesis and characterization of novel segmented polyurethane/clay nanocomposites. *Polymer* 2000; 41(4): 1345–1353.
17. Chen-Yang YW, Lee YK, Chen YT and Wu JC. High improvement in the properties of exfoliated PU/clay nanocomposites by the alternative swelling process. *Polymer* 2007; 48(10): 2969–2979.
18. Chen-Yang YW, Yang HC, Li GJ and Li YK. Thermal and anticorrosive properties of polyurethane/clay nanocomposites. *J Polym Res* 2004; 11(4): 275–283.
19. Choi WJ, Kim SH, Kim YJ and Kim SC. Synthesis of chain-extended organifier and properties of polyurethane/clay nanocomposites. *Polymer* 2004; 45(17): 6045–6057.
20. Dan CH, Lee MH, Kim YD, Min BH and Kim JH. Effect of clay modifiers on the morphology and physical properties of thermoplastic polyurethane/clay nanocomposites. *Polymer* 2006; 47(19): 6718–6730.
21. Finnigan B, Martin D, Halley P, Truss R and Campbell K. Morphology and properties of thermoplastic polyurethane nanocomposites incorporating hydrophilic layered silicates. *Polymer* 2004; 45(7): 2249–2260.
22. Finnigan B, Martin D, Halley P, Truss R and Campbell K. Morphology and properties of thermoplastic polyurethane composites incorporating hydrophobic layered silicates. *J Appl Polym Sci* 2005; 97(1): 300–309.
23. Gorrasi G, Tortora M and Vittoria V. Synthesis and physical properties of layered silicates/polyurethane nanocomposites. *J Polym Sci, Part B: Polym Phys* 2005; 43(18): 2454–2467.
24. Han B, Cheng AM, Ji GD, Wu SS and Shen J. Effect of organophilic montmorillonite on polyurethane/montmorillonite nanocomposites. *J Appl Polym Sci* 2004; 91(4): 2536–2542.
25. Hu Y, Song L, Xu J, Yang L, Chen Z and Fan W. Synthesis of polyurethane/clay intercalated nanocomposites. *Colloid Polym Sci* 2001; 279(8): 819–822.
26. Jiang HB, Oian JW, Bai YX, Fang MH and Qian XQ. Preparation and properties of polyurethane/montmorillonite nanocomposites cured under room temperature. *Polym Compos* 2006; 27(5): 470–474.
27. Jin J, Song M, Yao KJ and Chen L. A study on viscoelasticity of polyurethane-organoclay nanocomposites. *J Appl Polym Sci* 2006; 99(6): 3677–3683.
28. Kim BK, Seo JW and Jeong HM. Morphology and properties of waterborne polyurethane/clay nanocomposites. *Eur Polym J* 2003; 39(1): 85–91.
29. Kim DS, Kim JT and Woo WB. Reaction kinetics and characteristics of polyurethane/clay nanocomposites. *J Appl Polym Sci* 2005; 96(5): 1641–1647.
30. Ma JS, Zhang SF and Qi ZN. Synthesis and characterization of elastomeric polyurethane/clay nanocomposites. *J Appl Polym Sci* 2001; 82(6): 1444–1448.
31. Ma XY, Lu HJ, Lian GZ, Zhao JC and Lu TL. Rectorite/thermoplastic polyurethane nanocomposites. II. Improvement of thermal and oil-resistant properties. *J Appl Polym Sci* 2005; 96(4): 1165–1169.

32. Moon SY, Kim JK, Nah C and Lee YS. Polyurethane/montmorillonite nanocomposites prepared from crystalline polyols, using 1,4-butanediol and organoclay hybrid as chain extenders. *Eur Polym J* 2004; 40(8): 1615–1621.
33. Ni P, Li J, Suo JS and Li SB. Novel polyether polyurethane/clay nanocomposites synthesized with organic-modified montmorillonite as chain extenders. *J Appl Polym Sci* 2004; 94(2): 534–541.
34. Pattanayak A and Jana SC. High-strength and low-stiffness composites of nanoclay-filled thermoplastic polyurethanes. *Polym Eng Sci* 2005; 45(11): 1532–1539.
35. Pattanayak A and Jana SC. Thermoplastic polyurethane nanocomposites of reactive silicate clays: effects of soft segments on properties. *Polymer* 2005; 46(14): 5183–5193.
36. Pattanayak A and Jana SC. Synthesis of thermoplastic polyurethane nanocomposites of reactive nanoclay by bulk polymerization methods. *Polymer* 2005; 46(10): 3275–3288.
37. Pattanayak A and Jana SC. Properties of bulk-polymerized thermoplastic polyurethane nanocomposites. *Polymer* 2005; 46(10): 3394–3406.
38. Pohl MM, Seefeld V and Mix R. TEM studies on nanocomposites of montmorillonite and polyurethane. *Eur J Cell Biol* 1997; 74: 125.
39. Rehab A, Akelah A, Agag T and Shalaby N. Preparation and characterization of polyurethane-organoclay nanocomposites. *Polym Compos* 2007; 28(1): 108–115.
40. Rehab A and Salahuddin N. Nanocomposite materials based on polyurethane intercalated into montmorillonite clay. *Mater Sci Eng A* 2005; 399(1–2): 368–376.
41. Rhoney I, Brown S, Hudson NE and Pethrick RA. Influence of processing method on the exfoliation process for organically modified clay systems. I. Polyurethanes. *J Appl Polym Sci* 2004; 91(2): 1335–1343.
42. Song L, Hu Y, Tang Y, Zhang R, Chen ZY and Fan WC. Study on the properties of flame retardant polyurethane/organoclay nanocomposite. *Polym Degrad Stab* 2005; 87(1): 111–116.
43. Song M, Hourston DJ, Yao KJ, Tay JKH and Ansarifar MA. High performance nanocomposites of polyurethane elastomer and organically modified layered silicate. *J Appl Polym Sci* 2003; 90(12): 3239–3243.
44. Tien YI and Wei KH. The effect of nano-sized silicate layers from montmorillonite on glass transition, dynamic mechanical, and thermal degradation properties of segmented polyurethane. *J Appl Polym Sci* 2002; 86(7): 1741–1748.
45. Tortora M, Gorrasi G, Vittoria V, Galli G, Ritrovati S and Chiellini E. Structural characterization and transport properties of organically modified montmorillonite/polyurethane nanocomposites. *Polymer* 2002; 43(23): 6147–6157.
46. Varghese S, Gatos KG, Apostolov AA and Karger-Kocsis J. Morphology and mechanical properties of layered silicate reinforced natural and polyurethane rubber blends produced by latex compounding. *J Appl Polym Sci* 2004; 92(1): 543–551.
47. Wang JC, Chen YH and Chen RJ. Preparation of thermosetting polyurethane nanocomposites by montmorillonite modified with a novel intercalation agent. *J Polym Sci, Part B: Polym Phys* 2007; 45(5): 519–531.
48. Wang JC, Chen YH and Wang JL. Preparation and properties of a novel elastomeric polyurethane/organic montmorillonite nanocomposite. *J Appl Polym Sci* 2006; 99(6): 3578–3585.
49. Wang JC, Chen YH and Wang YQ. Preparation and characterization of novel organic montmorillonite-reinforced blocked polyurethane nanocomposites. *Polym Polym Compos* 2006; 14(6): 591–601.
50. Xia HS, Shaw SJ and Song M. Relationship between mechanical properties and exfoliation degree of clay in polyurethane nanocomposites. *Polym Int* 2005; 54(10): 1392–1400.
51. Xia HS and Song M. Intercalation and exfoliation behaviour of clay layers in branched polyol and polyurethane/clay nanocomposites. *Polym Int* 2006; 55(2): 229–235.
52. Xiong JW, Liu YH, Yang XH and Wang XL. Thermal and mechanical properties of polyurethane/montmorillonite nanocomposites based on a novel reactive modifier. *Polym Degrad Stab* 2004; 86(3): 549–555.
53. Xiong JW, Zheng Z, Jiang HM, Ye SF and Wang XL. Reinforcement of polyurethane composites with an organically modified montmorillonite. *Composites Part A* 2007; 38(1): 132–137.
54. Yao KJ, Song M, Hourston DJ and Luo DZ. Polymer/layered clay nanocomposites: 2 polyurethane nanocomposites. *Polymer* 2002; 43(3): 1017–1020.
55. Zha WB, Choi S, Lee KM and Han CD. Dispersion characteristics of organoclay in nanoc omposites based on end-functionalized homopolymer and block copolymer. *Macromolecules* 2005; 38(20): 8418–8429.
56. Zhang XM, Xu RJ, Wu ZG and Zhou CX. The synthesis and characterization of polyurethane/clay nanocomposites. *Polym Int* 2003; 52(5): 790–794.
57. Zheng JR, Ozisik R and Siegel RW. Phase separation and mechanical responses of polyurethane nanocomposites. *Polymer* 2006; 47(22): 7786–7794.
58. Wang Z and Pinnavaia TJ. Nanolayer reinforcement of elastomeric polyurethane. *Chem Mater* 1998; 10(12): 3769–3771.
59. Solarski S, Benali S, Rochery M, Devaux E, Alexandre M, Monteverde F, et al. Synthesis of a polyurethane/clay nanocomposite used as coating: Interactions between the counterions of clay and the isocyanate and incidence on the nanocomposite structure. *J Appl Polym Sci* 2005; 95(2): 238–244.
60. Subramani S, Lee JM, Kim JH and Cheong IW. One-pack cross-linkable waterborne methyl ethyl ketoxime-blocked polyurethane/clay nanocomposite dispersions. *Macromol Res* 2005; 13(5): 418–426.
61. Pegoretti A, Dorigato A and Penati A (eds). Production and characteization of polyurethane-clay nanocomposites. In: *2nd International Symposium on Nanostructured and Functional Polymer-based Materials and Nanocomposites*, Lyon, France, 2006.
62. Pegoretti A, Dorigato A, Brugnara M and Penati A. Contact angle measurements as a tool to investigate the filler–matrix interactions in polyurethane–clay

nanocomposites from blocked prepolymer. *Eur Polym J* 2008; 44: 1662–1672.
63. Pegoretti A, Dorigato A and Penati A. Tensile mechanical response of polyethylene – clay nanocomposites. *Express Polym Lett* 2007; 1(3): 123–131.
64. Berta M, Saiani A, Lindsay C and Gunaratne R. Effect of clay dispersion on the rheological properties and flammability of polyurethane-clay nanocomposite elastomers. *J Appl Sci* 2009; 112: 2847–2853.
65. Maji PK, Guchhait PK and Bhowmick AK. Effect of nanoclays on physico-mechanical properties and adhesion of polyester-based polyurethane nanocomposites: structure–property correlations. *J Mater Sci* 2009; 44: 5861–5871.
66. Corcione CE, Prinari P, Cannoletta D, Mensitieri G and Maffezzoli A. Synthesis and characterization of clay-nanocomposite solvent-based polyurethane adhesives. *Int J Adhes Adhes* 2008; 28: 91–100.
67. Fereidoonnia M, Barmar M and Barikani M. Influence of a reactive organoclay on polymerization and properties of polyurethane nanocomposites. *Polym Plast Technol Eng* 2009; 48: 90–96.
68. Khudyakov IV, Zopf RD and Turro NJ. Polyurethane nanocomposites. *Des Monomers Polym* 2009; 12: 279–290.
69. Pizzatto L, Lizot A, Fiorio R, Amorim CL, Machado G, Giovanela M, et al. Synthesis and characterization of thermoplastic polyurethane/nanoclay composites. *Mater Sci Eng C* 2009; 29: 474–478.
70. Zou H, Ran Q, Wu S and Shen J. Study of nanocomposites prepared by melt blending TPU and montmorillonite. *Polym Compos* 2008; 29: 385–389.
71. Ajayan PM, Schadler LS and Braun PV. *Nanocomposite science and technology*. Weinhein: Wiley-VCH, 2003.
72. Alexandre M and Dubois P. Polymer-layered silicate nanocomposites: preparation, properties and uses of a new class of materials. *Mater Sci Eng* 2000; 28: 1–63.
73. Akbari B and Bagheri R. Deformation mechanism of epoxy/clay nanocomposite. *Eur Polym J* 2007; 43: 782–788.
74. Basara C, Yilmazer U and Bayram G. Synthesis and characterization of epoxy based nanocomposites. *J Appl Polym Sci* 2005; 98: 1081–1086.
75. Wang CH, Auad ML, Marcovich NE and Nutt S. Synthesis and characterization of organically modified attapulgite/polyurethane nanocomposites. *J Appl Polym Sci* 2008; 109: 2562–2570.
76. Kim TK, Kim BK, Kim YS, Cho YL, Lee SY, Cho YB, et al. The properties of reactive hot melt polyurethane adhesives: effects of molecular weight and reactive organoclay. *Polym Plast Technol Eng* 2009; 48: 932–938.
77. Dick JS and Annicelli RA (eds). *Rubber technology: Compounding and testing for perfomance*. Munich: Carl H Verlag, 2001.
78. Payne AR. *Reinforcement of elastomers*. New York: Interscience, 1965.
79. Cassagnau P. Payne effect and shear elasticity of silica-filled polymers in concentrated solutions and in molten state. *Polymer* 2003; 44: 2455–2462.
80. Payne AR. The dynamic properties of carbon black-loaded natural rubber vulcanizates. Part I. *J Appl Polym Sci* 1962; 6(19): 57–63.
81. Gauthier C, Reynaud E, Vassoille R and Ladouce-Stelandre L. Analysis of the non-linear viscoelastic behaviour of silica filled styrene butadiene rubber. *Polymer* 2004; 45: 2761–2771.
82. Jia Q, Wu YP, Wang YQ, Lu M, Yang J and Zhang LQ. Organic interfacial tailoring of styrene butadiene rubber–clay nanocomposites prepared by latex compounding method. *J Appl Polym Sci* 2007; 103: 1826–1833.
83. Wu YP, Wang YQ, Zhang HF, Wang YZ, Yu DS, Zhang LQ, et al. Rubber–pristine clay nanocomposites prepared by co-coagulating rubber latex and clay aqueous suspension. *Compos Sci Technol* 2005; 65: 1195–1202.